

Supporting Information (SI) for “An Alternative Approach to Estimate Solute Concentration: Exploiting the Information Embedded in the Solid Phase”

Stefan Bötschi,^{a‡} Ashwin Kumar Rajagopalan,^{a‡} Manfred Morari,^b and
Marco Mazzotti^{*a}

In this supporting material, we provide additional information on the materials, on the experimental setup, on the experimental protocol employed in this work, as well as a qualitative comparison of the concentration estimate obtained using ATR-FTIR and the stereoscopic imaging device μ -DISCO. An elementary error analysis is also presented that sheds light on how uncertainties in the measured total visual hull volume translate into errors in the concentration estimate when using the μ -DISCO.

In section 1, the materials used in the experiments, a description of the μ -DISCO setup, and the seed preparation protocol for both BLGA and vanillin are reported. In section 2, the experimental protocol to estimate the solubility curves is explained for both compounds, and a table listing all the experiments performed in the scope of this work is provided. In section 3, a qualitative comparison of the solubility curve obtained using the ATR-FTIR technique and the μ -DISCO is presented for BLGA in water in a predefined temperature range. Finally, in section 4, the elementary error analysis is discussed.

1 Materials and Methods

1.1 Materials

Monosodium L-glutamic acid monohydrate (NaGlu, Sigma-Aldrich, Buchs, Switzerland, purity > 99 %) and hydrochloric acid (HCl, Sigma-Aldrich, Buchs, Switzerland, 37-38 %) were used as purchased to prepare seed crystals. For all the experiments performed in the scope of this work, deionized and filtered (filter size of 0.22 μ m) water was taken from a Milli-Q Advantage A10 system (Millipore, Zug, Switzerland). The needle-like, stable β polymorph of L-glutamic acid was used for the experiments involving this compound. The saturated solutions were prepared using β L-glutamic acid (BLGA, Sigma-Aldrich, Buchs, Switzerland, purity > 99 %). The BLGA crystals purchased from the manufacturer were not used for seeding the experiments. Instead, a seed preparation protocol, which is described in section 1.3, was employed.

Vanillin (Sigma-Aldrich, Buchs, Switzerland) and deionized and filtered water were used for the experiments. Four different polymorphs of Vanillin exist. The stable form I was purchased from the supplier and subsequently used as purchased for the preparation of saturated solution and seed crystals.

^a *Institute of Process Engineering, ETH Zurich, 8092 Zurich, Switzerland. E-mail: marco.mazzotti@ipe.mavt.ethz.ch. Telephone: +41 44 632 24 56. Fax: +41 44 632 11 41.*

^b *Department of Electrical and Systems Engineering, University of Pennsylvania, Philadelphia 19104, United States.*

[‡] These authors contributed equally to this work.

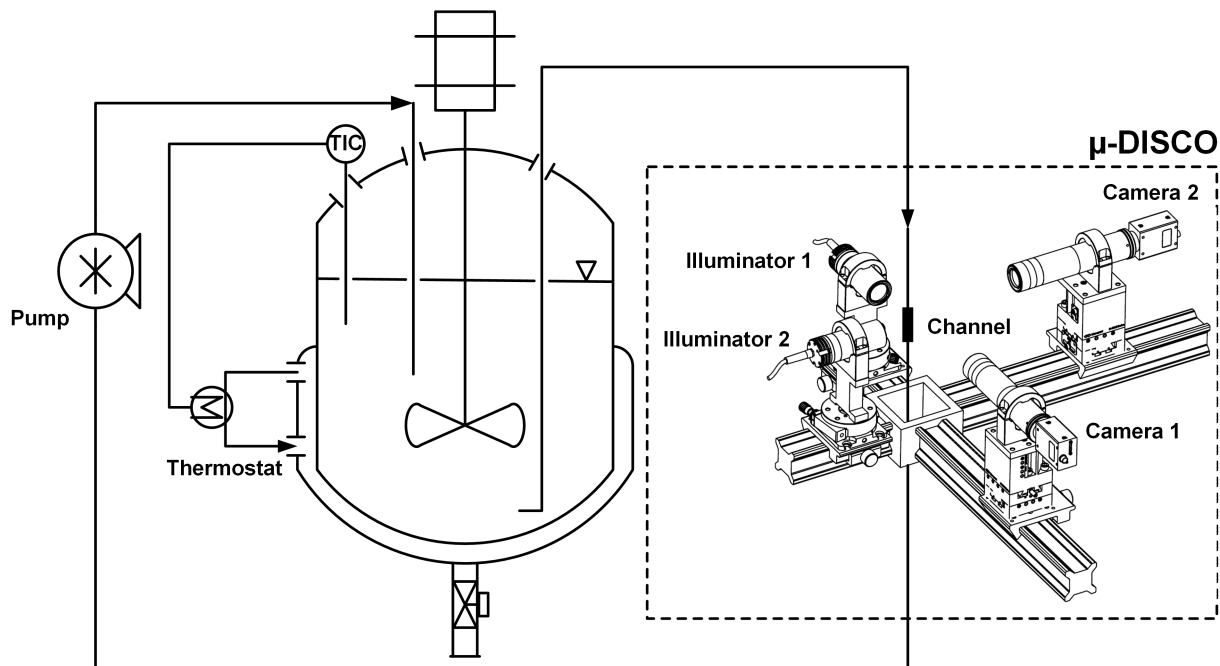


Figure 1: Schematic of the experimental setup (crystallizer and sampling loop) coupled with the stereoscopic imaging device (μ -DISCO). A predefined temperature profile for each experiment is provided to the thermostat, which in turn controls the temperature of the suspension.

1.2 Setup

The experiments in this work were performed in a 2000 mL glass jacketed stirred crystallizer. A ministat 230-CC3 thermostat (Huber, Offenburg, Germany) was used to control the temperature in the crystallizer, where the controller parameters were fixed at P-cascade = 1000, I-cascade = 750, D-cascade = 0. The suspension for all the experiments was stirred at 400 rpm using a 4-blade glass impeller of 60 mm diameter at an inclination of 45° (LaboTechSystems LTS AG, Reinach, Switzerland). As briefly discussed in the main text, the characterization of the solid phase was performed using the stereoscopic imaging device μ -DISCO¹, which is an *ex situ* device that makes use of a sampling loop; a schematic of this setup is shown in Figure 1.

The suspension from the crystallizer was pumped through a square channel at a flow rate of 400 mL min^{-1} . Every 2 min, either 500 or 800 images of the suspension were acquired at a frequency of around 75 frames per second. During the image acquisition phase, the flow rate was reduced to 100 mL min^{-1} to avoid motion blur. The images obtained were processed using an automated image analysis routine to characterize the solid phase, i.e., to obtain a multidimensional particle size and shape distribution (PSSD). Apart from characterizing the dimensions of the particles, the μ -DISCO provides also an estimate of the volume of the crystals being sampled from the crystallizer, referred to as the total visual hull volume in the main text. Within the scope of this work, the total visual hull volume is the measured quantity of interest and the visual hull volume of each observed crystal was considered. Further information regarding the μ -DISCO and the image analysis routines can be found elsewhere.¹

1.3 Seed Preparation Protocol

In the case of BLGA, the seed crystals were prepared by means of a two-step pH-shift precipitation. In the first step, crystals of the α polymorph of L-Glutamic acid (ALGA) were produced by mixing equimolar quantities of NaGlu and HCl in deionized and filtered water and by stirring at 300 rpm at 5.0 °C for 1 h. Subsequently, the solution was filtered off and the ALGA crystals were dried. In the second step, a saturated solution of ALGA in water at 45.0 °C was prepared by again mixing equimolar quantities of NaGlu and HCl. The ALGA crystals obtained in the previous step were suspended in this solution and subsequently allowed to undergo a solvent-mediated polymorphic transformation to the β polymorph.² The solution was filtered off, the BLGA crystals were dried, and finally, they were dry-sieved using the sieve fraction 90-180 μm .

In the case of vanillin, a saturated solution of vanillin in water was prepared at 40 °C, corresponding to a concentration of 23.49 g kg⁻¹ on a per mass of solvent basis. The saturated solution was subsequently crash-cooled to 20 °C. Once the temperature reached 20 °C, the suspension was filtered off and the retained solids were dried.

2 Experimental Protocol

2.1 BLGA

For the five BLGA experiments discussed in the main part of this article (and referred to as experiment α through ϵ), saturated solutions of BLGA in water were prepared at the temperatures 25.0 °C, 25.8 °C, 27.0 °C, 28.2 °C, and 29.4 °C by adding excess amounts of purchased BLGA and letting the suspensions equilibrate for several hours. Afterwards, for each experiment, the solution was filtered off and 2000.0 g were loaded into the batch crystallizer. The sampling loop of the μ -DISCO was inserted into the crystallizer, and the clear solution was cooled down to the temperature corresponding to the desired initial supersaturation of 1.01. Upon reaching this temperature, 0.8 g of BLGA seed crystals were added to the clear solution. Subsequently, the following temperature profile was applied to the suspension: first, it was kept at the initial temperature for two hours, i.e., at slightly supersaturated conditions. This ensured that the solid particles did not dissolve during this initial phase. Note that the growth rate of BLGA at such a low supersaturation is negligible. Then, a heating rate of 0.3 °C h⁻¹ was applied until reaching the saturation temperature, where the suspension was kept for half an hour. Subsequently, the suspension was heated again with a heating rate of 0.3 °C h⁻¹ for two hours, after which it was kept at the intermediate temperature for either half an hour or two hours (intermediate temperature plateau), before heating it further with the same heating rate until it reached the final temperature of the experiment, which was 1.2 °C above the saturation temperature. Finally, the suspension was kept at the final temperature for either two or five hours. The duration of this final phase, of the intermediate temperature plateau, as well as the initial temperature T_0 , the saturation temperature T_{sat} , and the final temperature T_{final} are listed in Table 1 for each experiment discussed in the main text. In addition to these five experiments, another experiment was performed that covered the temperature range from 26.2 °C to 27.4 °C (experiment ζ) using the same protocol as described above. This experiment can be seen as a reproducibility test since it covered a temperature interval that was already covered by the series of experiments α through ϵ . The corresponding data, alongside the data of the five main experiments, are visualized in Figure 2a in the form of a concentration versus temperature plot; the

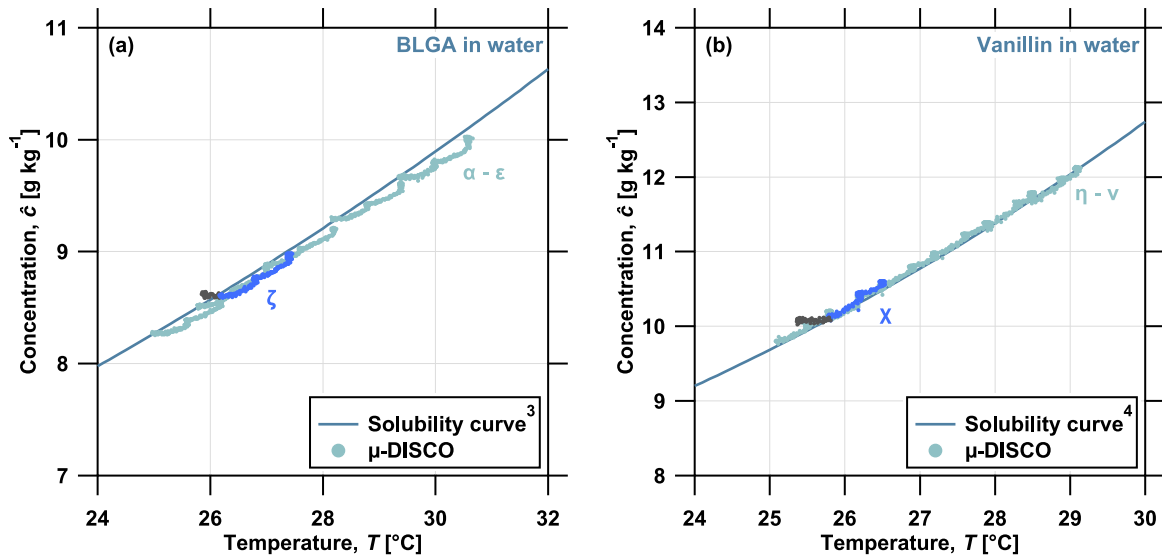


Figure 2: (a) Solubility curve of BLGA in water reported in the literature³ (solid blue line), and concentration estimated using the μ -DISCO for experiments α through ϵ (light blue solid markers) and ζ (dark gray and dark blue solid markers). The dark gray markers highlight the data points of experiment ζ where the temperature was below the initial saturation temperature T_{sat} . (b) Solubility curve of vanillin in water reported in the literature⁴ (solid blue line), and concentration estimated using the μ -DISCO for experiments η through ν (light blue solid markers) and χ (dark gray and dark blue solid markers). The dark gray markers highlight the data points of experiment χ where the temperature was below the initial saturation temperature T_{sat} .

key parameters of experiment ζ are also reported in Table 1.

2.2 Vanillin

For the six vanillin experiments discussed in the main part of this article (and referred to as experiment η through ν), saturated solutions of vanillin in water were prepared at the temperatures 25.1 °C, 25.8 °C, 26.5 °C, 27.2 °C, 27.9 °C, and 28.5 °C by adding excess amounts of purchased vanillin and letting the suspensions equilibrate for several hours. Afterwards, for each experiment, the solution was filtered off and 2000.0 g were loaded into the batch crystallizer. The sampling loop of the μ -DISCO was inserted into the crystallizer, and the clear solution was cooled down to the temperature corresponding to the desired initial supersaturation of 1.02. Upon reaching this temperature, 1.0 g of vanillin seed crystals were added to the clear solution. Subsequently, the following temperature profile was applied to the suspension: first, it was kept at the initial temperature for three and a half hours. The vanillin seeds used for the experiments were aggregated and suspending them in water led to a detectable deaggregation over a period of about 90 min, during which also the observed total visual hull volume stabilized. This initial stabilization phase was removed from the data in a post-processing step. Similar to BLGA, during the initial phase, the suspension was under slightly supersaturated conditions, and growth of the crystals was not observed during this phase. After staying at the initial temperature, a heating rate of 0.3 °C h⁻¹ was applied until reaching the saturation temperature, where the suspension was kept for 30 min. Subsequently, the suspension was heated again with a heating rate of 0.3 °C h⁻¹ for 80 min, after which it was kept at the intermediate temperature for 2 h (intermediate temperature plateau), before heating it further with the same heating rate until it reached the final temperature of

the experiment. This final temperature was either 0.7 °C (experiments η - κ) or 0.6 °C (experiments λ and ν) above the saturation temperature. Finally, the suspension was kept at the final temperature for another 5 h. The duration of this final phase, of the intermediate temperature plateau, as well as the initial temperature T_0 , the saturation temperature T_{sat} , and the final temperature T_{final} are listed in Table 1 for each experiment discussed in the main text. In addition to these six experiments, another experiment was performed that covered the temperature range from 25.8 °C to 26.5 °C (experiment χ) using the same protocol as described above, i.e., this experiment can be seen as a repetition of experiment θ . The corresponding data, alongside the data of the six main experiments, are visualized in Figure 2b in the form of a concentration versus temperature plot.

Table 1: Experimental conditions explored to estimate the solubility curves of BLGA in water and of vanillin in water using the method proposed in this work.

Exp	Intermediate plateau duration [h]	Final phase duration [h]	T_0 [°C]	T_{sat} [°C]	T_{final} [°C]
BLGA					
α	2.0	5.0	24.7	25.0	26.2
β	0.5	2.0	25.5	25.8	27.0
γ	0.5	2.0	26.7	27.0	28.2
δ	2.0	5.0	27.9	28.2	29.4
ϵ	2.0	5.0	29.1	29.4	30.6
ζ	2.0	5.0	25.9	26.2	27.4
Vanillin					
η	2.0	5.0	24.7	25.1	25.8
θ	2.0	5.0	25.4	25.8	26.5
ι	2.0	5.0	26.1	26.5	27.2
κ	2.0	5.0	26.8	27.2	27.9
λ	2.0	5.0	27.5	27.9	28.5
ν	2.0	5.0	28.1	28.5	29.1
χ	2.0	5.0	25.4	25.8	26.5

3 Comparison Between Concentration Estimates Based on ATR-FTIR Spectroscopy and on Stereoscopic Imaging

As discussed in the main text, ATR-FTIR spectroscopy is one of the the most commonly used techniques to monitor the solute concentration in a crystallization process. In order to better understand the shortcomings of using ATR-FTIR to measure the concentration for systems that are challenging, a study was performed to compare the solubility curve measurements obtained from the ATR-FTIR with the method proposed in this work. To this end, the solubility of BLGA in water was measured experimentally using a ReactIR 45m system from Mettler-Toledo (Greifensee, Switzerland), equipped with a diamond ATR crystal. The spectra were collected over a 1 min interval in the range 650 cm^{-1} to

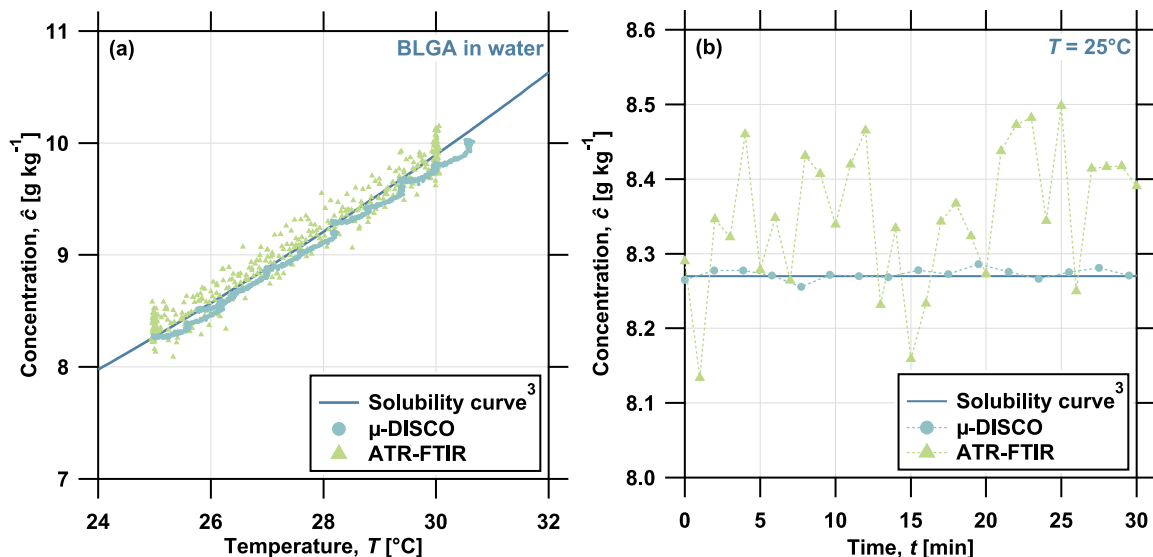


Figure 3: (a) Solubility curve of BLGA in water reported in the literature³ (solid blue line), measured using the μ -DISCO (light blue solid markers), and ATR-FTIR (light green solid markers). (b) Solubility of BLGA in water at 25 °C reported in the literature³ (solid blue line) and evolution of the concentration of BLGA in water measured at constant temperature using the μ -DISCO (light blue solid markers) and using ATR-FTIR (light green solid markers).

2400 cm⁻¹ with a resolution of 4 cm⁻¹. A linear baseline correction and Savitzky-Golay filtering were applied to all the spectra. The linear baseline consisted of a linear spline, spanning the wavenumber ranges from 1208 cm⁻¹ to 1240 cm⁻¹ and from 1336 cm⁻¹ to 1476 cm⁻¹. A multivariate calibration model based on the partial least squares method with 49 variables was built using known concentrations,⁵ and this model was subsequently used for estimating the solubility curve.

When the ATR-FTIR was used, the solubility of BLGA in water was measured by heating a saturated suspension from 25 °C to 30 °C at a rate of 1 °C h⁻¹. At 25 °C and at 30 °C, the temperature was held constant to verify if the suspension was at equilibrium. An excess of solid particles was added at the beginning of the experiment to ensure that the suspension would also be at equilibrium at the end of the experiment. Since a single experiment was used to cover the whole temperature range between 25 °C to 30 °C, this implies that the solid phase concentration in this experiment was considerably higher than the one in the experiments where the μ -DISCO was applied to estimate the solute concentration.

For obtaining the concentration estimates using stereoscopic imaging,³ the protocol described in section 2 was employed.

The solubility curve of BLGA in water estimated using the μ -DISCO (experiments α - ϵ), the one obtained from ATR-FTIR, and the solubility curve reported in the literature³ are shown in Figure 3a. One can infer from it that the concentration estimates of both techniques are in good agreement with the literature data. However, a closer look reveals a higher noise level in the concentration estimate obtained from ATR-FTIR when compared with the one obtained from the μ -DISCO over the whole temperature range explored. Time-resolved concentration estimates obtained from the μ -DISCO and from ATR-FTIR at a temperature plateau corresponding to 25 °C are shown in Figure 3b. Even though the concentration estimate obtained from ATR-FTIR has an error of less than 3% with respect to the equilibrium concentration reported in the literature, the estimated concentration at a constant temperature again confirms that the noise level from the ATR-FTIR is significantly higher than the one

obtained from the μ -DISCO in this case. Since the spectroscopic instrument was carefully calibrated using a state-of-the-art method,⁵ the higher noise level has to be attributed to the inherent limitations of the technique applied to this system (having low solubility and exhibiting a weak peak in the mid-IR region).

The comparison presented in this section indicates that a concentration estimate with a comparatively low noise level for the system BLGA in water was obtained using the μ -DISCO. However, the advantages that ATR-FTIR spectroscopy has over multiprojection imaging in terms of concentration estimation, besides being widely used, also need to be kept in mind. In fact, obtaining a solubility curve using IR spectroscopy enables exploring larger ranges of temperature and concentration in a single experiment, where the high solid phase concentration hinders covering the same range using a multiprojection imaging based method in the absence of additional dilution equipment. Moreover, ATR-FTIR spectroscopy has the ability to distinguish different species in solution. This information cannot be inferred from a multiprojection imaging device, since it only observes directly the solid phase.

For a crystallization experiment, be it either growth or dissolution, the imaging based method requires only knowledge of the equilibrium (or initial) solute phase concentration, thereby eliminating the need to build a calibration model. This feature is particularly beneficial since building a calibration model for a spectroscopic concentration measurement method requires a time-consuming series of experiments using comparatively large amounts of solid material.

4 Elementary Error Analysis

As discussed in the main text, estimating the solute concentration based on multiprojection imaging is not free of errors, and an experimental approach to quantify the overall inaccuracy is presented by means of measuring the solubility curves of two different compounds. An alternative way of assessing the impact of the first possible source of error mentioned in the main text, namely the uncertainty in the total visual hull volume, is to propagate the uncertainty in this measurement through eq 1 of the main text. As a first step, eq 3 of the main text is plugged into eq 1 of the main text, which yields

$$\hat{c}(t) = c_0 - \rho_c V_{\text{seed}} \left(\frac{\hat{V}(t)}{\hat{V}(t_0)} - 1 \right) \quad (1)$$

For the elementary error analysis discussed below, we make the simplifying assumption that c_0 , ρ_c , and V_{seed} are known exactly, whereas $\hat{V}(t)$ and $\hat{V}(t_0)$ are subject to uncertainty. In order to propagate the uncertainties in the latter two quantities through eq 1, they have to be known quantitatively, which is however not the case in reality. Thus, in this section, we rely on an *in silico* study to quantify the difference between the total visual hull volume $\hat{V}(t)$ measured by the stereoscopic imaging device μ -DISCO and the true total volume $V_{\text{true}}(t)$ of a sampled and observed subset of a population of polyhedral particles. To do so, both quantities were determined using the virtual test bench (VTB) introduced and applied previously.⁶⁻⁸ The purpose of the VTB is to emulate *in silico* the measurement process performed by a stereoscopic imaging device that relies on sampling of the suspension from a batch crystallizer. In general, it is a priori clear that the difference between the two quantities $V_{\text{true}}(t)$ and $\hat{V}(t)$ is a strong function of the actual geometry of the observed particles and also of their size, since these factors influence the accuracy of the visual hull approximation procedure.¹ Therefore, the error analysis was conducted for three different particle populations that were measured during three

different temperature plateaus of experiment α , which implies that the particle sizes in these three populations are different as well.

4.1 Measurement of Particle Populations

As discussed in section 1.2, the μ -DISCO characterizes the dimensions of the observed particles. For experiment α , about 85% of all observed particles were classified as either needle-like or quasi-equant by the automated shape classifier algorithm of the μ -DISCO¹. The characteristic dimensions of these particles were obtained by imposing a cylinder shape with a characteristic length and width. These dimensions were subsequently used to generate a 2D PSSD (henceforth referred to as PSSD).

In order to perform the error analysis, the particle population was obtained from the μ -DISCO for experiment α at three different temperature plateaus T_{sim} corresponding to 25.0 °C, 25.6 °C, and 26.2 °C. To obtain a statistically relevant number of particles, at each temperature plateau, the population was characterized using a sampling interval of 2 min over a period of 30 min. The resulting 15 measurements were concatenated to yield a single population, characteristic of each temperature plateau. A total of about 75 300, 67 700, and 60 100 particles were used to reconstruct the PSSD at a temperature of 25.0 °C, 25.6 °C, and 26.2 °C, respectively. Notice that, due to the dissolution of the crystals over time, the number of particles used to reconstruct the PSSDs reduces as the temperature increases for a fixed time of observation.

Since the PSSDs obtained in this way were based on the generic, cylindrical particle shape model, they were subsequently transformed into the polyhedral particle model for BLGA and they were scaled to match the solid mass present in the experiment, as described elsewhere.⁸

4.2 Quantification of the Uncertainty in the Total Visual Hull Volume

The three particle populations obtained as explained in section 4.1 were input to the simulation framework described previously.⁸ For each of these populations, a steady state simulation (i.e., at saturated conditions) over a duration of 5 h was conducted, where the saturation temperatures T_{sim} were given by 25.0 °C, 25.6 °C, and 26.2 °C, and the corresponding solubilities $c^*(T_{\text{sim}})$ were obtained from the solubility data reported in the literature.³ During these steady state simulations, in order to emulate the measurement process of the μ -DISCO, the particle populations were characterized using the VTB as described elsewhere⁸, with a sampling time of 2 min. The number of polyhedral BLGA particles N_s sampled at each sampling instant was 7000, 5742, and 4470 for the three populations. N_p of these particles were placed in the virtual flow channel at the same time, leading to N_s/N_p pairs of virtual images to be analyzed at each sampling instant. N_p was set to 14, 11, and 6. Note that the values chosen for N_s and N_p were inferred from the experimental data of experiment α . Both the total visual hull volume $\hat{V}(t)$ of the simulated measurement and the true total volume $V_{\text{true}}(t)$ of the sampled subset of polyhedral BLGA particles were computed. The evolution of $\hat{V}(t)$ and $V_{\text{true}}(t)$, as well as that of the ratio of these two quantities, is visualized in Figure 4 for the three steady-state simulations. It can be seen in Figure 4a that both $\hat{V}(t)$ and $V_{\text{true}}(t)$ exhibit small fluctuations around an otherwise constant level for all three cases. Additionally, it can also be observed that the level of both quantities decreases with increasing temperature, indicating the decrease in the overall particle volume caused by dissolution over the course of experiment α . Figure 4b demonstrates that the ratio of $\hat{V}(t)$ to $V_{\text{true}}(t)$ is larger than 1 for all three populations, i.e., the total visual hull volume always overestimates the true volume of the sampled particles. Furthermore, this ratio is also a function of the particle size, as indicated

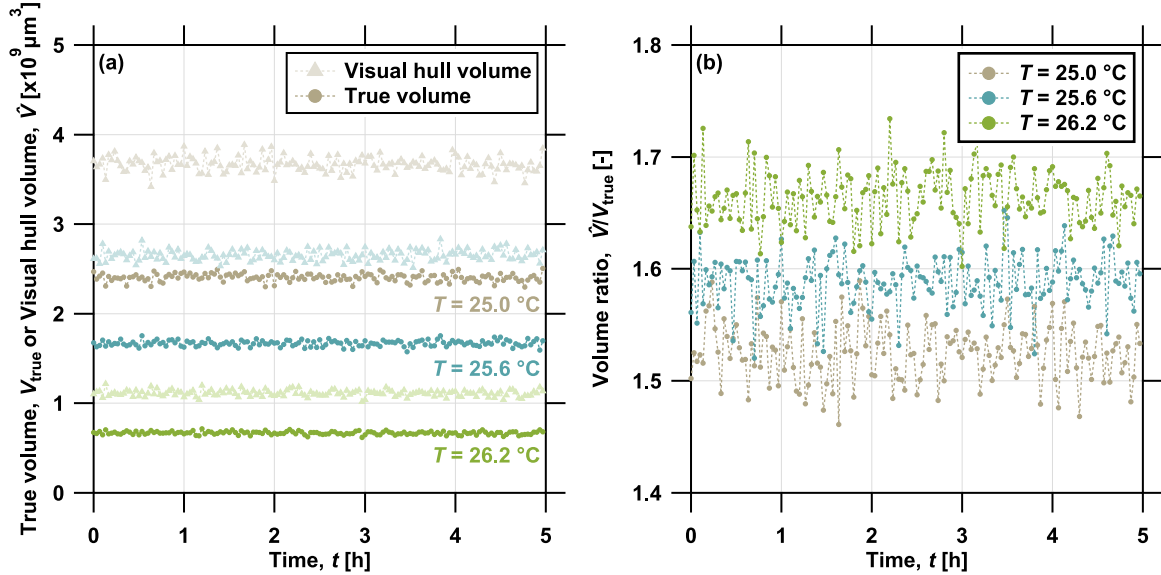


Figure 4: **(a)** Evolution of the true volume V_{true} of the sampled particles (dark lines with circular markers) and of the total visual hull volume \hat{V} of the observed particles (light lines with triangular markers) for the three steady state simulations obtained from the VTB. **(b)** Evolution of the ratio of the total visual hull volume \hat{V} to the true volume of the sampled particles V_{true} for the three steady state simulations obtained from the VTB.

by the different temperature plateaus. The smaller the particles get (i.e., the higher the temperature plateau), the larger the ratio of $\hat{V}(t)$ to $V_{\text{true}}(t)$ gets. In other words, the relative overestimation of the particle volume by the visual hull gets larger as the particle size decreases.

4.3 Error Propagation and Results

The uncertainty in the observed particle volume (as quantified in section 4.2) needs to be propagated through eq 1 to assess the impact that it has on the concentration estimate \hat{c} . Two different types of errors need to be analyzed:⁹ first, the random error that stems from the fluctuations in the data (see Figure 4a), and second, the systematic error that arises as a consequence of the deviation between $V_{\text{true}}(t)$ and $\hat{V}(t)$ (see Figure 4). To do so, as a first step, a number of key figures need to be derived from the data illustrated in Figure 4a. Concerning the uncertainty in $\hat{V}(t_0)$, we define

$$\begin{aligned} V_0 &:= \hat{V}_{25.0}(t_0) \\ \sigma_{V_0}^2 &:= \text{Var} \left[\hat{V}_{25.0}(t) \right] \end{aligned} \quad (2)$$

i.e., V_0 is the first measurement of the total visual hull volume obtained in the steady state simulation at 25.0°C and $\sigma_{V_0}^2$ is the empirical variance of the time-resolved total visual hull volume at 25.0°C , since in principle, due to the random sampling, the variance of V_0 and the variance of the time-resolved total visual hull at the desired temperature should be equal. Concerning $\hat{V}(t)$, we define the two statistical measures

$$\begin{aligned} \bar{V}_{T_{\text{sim}}} &:= \text{E} \left[\hat{V}_{T_{\text{sim}}}(t) \right] \\ \sigma_{V_{T_{\text{sim}}}}^2 &:= \text{Var} \left[\hat{V}_{T_{\text{sim}}}(t) \right] \end{aligned} \quad (3)$$

where T_{sim} is either 25.0 °C, 25.6 °C, or 26.2 °C. In eq 3, $\bar{V}_{T_{\text{sim}}}$ is the mean value of the time-resolved total visual hull volume observed in the steady-state simulation conducted at T_{sim} and $\sigma_{V_{T_{\text{sim}}}}^2$ is the variance of the same quantity.

By the propagation of error formulas,⁹ the mean \bar{c} and the variance $\sigma_{\hat{c}}^2$ of the concentration estimate \hat{c} in steady-state at T_{sim} can be approximated by

$$\begin{aligned}\bar{c} &= c_0 - \rho_c V_{\text{seed}} \left(\frac{\bar{V}_{T_{\text{sim}}}}{V_0} - 1 \right) \\ \sigma_{\hat{c}}^2 &= \left(\frac{\partial \hat{c}}{\partial \hat{V}} \Big|_{V_0, \bar{V}_{T_{\text{sim}}}} \right)^2 \sigma_{V_{T_{\text{sim}}}}^2 + \left(\frac{\partial \hat{c}}{\partial \hat{V}_0} \Big|_{V_0, \bar{V}_{T_{\text{sim}}}} \right)^2 \sigma_{V_0}^2 \\ &= \rho_c^2 V_{\text{seed}}^2 \left(\frac{1}{V_0^2} \sigma_{V_{T_{\text{sim}}}}^2 + \frac{\bar{V}_{T_{\text{sim}}}^2}{V_0^4} \sigma_{V_0}^2 \right)\end{aligned}\quad (4)$$

where \hat{V}_0 is a placeholder for $\hat{V}(t_0)$. Equation 4 accounts for the impact of two random errors: first, for the fact that V_0 solely depends on the random sampling of the particle population at the first sampling instant of an experiment (here: at 25.0 °C). Second, eq 4 also accounts for the random fluctuations of \hat{V} (see Figure 4a), whose impact on the concentration estimate is quantified by $\sigma_{\hat{c}}^2$.

As can be seen in Figure 4, the total visual hull volume consistently overestimates the true volume of the sampled particles. As long as this overestimation is consistent between $\hat{V}(t_0)$ and $\hat{V}(t)$, it does not introduce a bias in the concentration estimate, since only the ratio of these two quantities is considered in eq 1. However, as the particles change in size, $\bar{V}_{T_{\text{sim}}}$ overestimates the true volume of the particles by a different factor, as can be seen in Figure 4b. Since the volume overestimation associated with V_0 remains the same for all the three temperature plateaus considered in this study, a bias or a systematic error⁹ is introduced in the concentration estimate. This systematic error can be quantified by

$$\Delta \hat{c} := c^*(T_{\text{sim}}) - \bar{c} = c^*(T_{\text{sim}}) - c_0 + \rho_c V_{\text{seed}} \left(\frac{\bar{V}_{T_{\text{sim}}}}{V_0} - 1 \right) \quad (5)$$

where the true concentration $c^*(T_{\text{sim}})$ at the considered temperature plateau T_{sim} is known.

When applying Eqs. 2 through 5 to the data obtained from the *in silico* study presented in this section, the numerical values listed in Table 2 are obtained. The true concentration $c^*(T_{\text{sim}})$ (corresponding to thermodynamic equilibrium or steady state) obviously increases with the temperature T_{sim} . The mean \bar{c} of the concentration estimate is close to the true concentration $c^*(T_{\text{sim}})$ in all three cases. The standard deviation $\sigma_{\hat{c}}$ of the concentration estimate decreases slightly with increasing temperature, which is consistent with the fluctuations of the total visual hull volume visualized in Figure 4a. As expected from the explanation given above, the systematic error $\Delta \hat{c}$ increases with increasing temperature. Also, it is worth noting that the magnitude of the uncertainties in the first row of Table 2 is consistent with the experimentally observed uncertainty at the temperature plateau of 25.0 °C as illustrated in Figure 3b. To conclude, it can be said that both the random and the systematic error in the concentration estimate are small in magnitude.

Table 2: True concentration $c^*(T_{\text{sim}})$, mean \bar{c} and standard deviation $\sigma_{\hat{c}}$ of the concentration estimate, and systematic error $\Delta\hat{c}$ obtained from the elementary error analysis conducted for all the three temperatures plateaus T_{sim} considered in the *in silico* study.

T_{sim} [°C]	$c^*(T_{\text{sim}})$ [g kg ⁻¹]	\bar{c} [g kg ⁻¹]	$\sigma_{\hat{c}}$ [g kg ⁻¹]	$\Delta\hat{c}$ [g kg ⁻¹]
25.0	8.268	8.272	0.013	-0.004
25.6	8.448	8.383	0.009	0.066
26.2	8.632	8.550	0.005	0.082

The accurate estimation of the solubility curves for the two compounds, the qualitative analysis presented in section 3, and the error analysis presented in this section clearly indicate that the concentration estimation technique presented in this work can be used quantitatively in a seeded batch crystallization or dissolution process.

References

- [1] Rajagopalan, A. K.; Schneeberger, J.; Salvatori, F.; Bötschi, S.; Ochsenein, D. R.; Oswald, M. R.; Pollefeys, M.; Mazzotti, M. A comprehensive shape analysis pipeline for stereoscopic measurements of particulate populations in suspension. *Powder Technol.* **2017**, *321*, 479–493.
- [2] Cornel, J.; Lindenberg, C.; Mazzotti, M. Experimental Characterization and Population Balance Modeling of the Polymorph Transformation of L-Glutamic Acid. *Cryst. Growth Des.* **2009**, *9*, 243–252.
- [3] Schöll, J.; Bonalumi, D.; Vicum, L.; Mazzotti, M.; Müller, M. In Situ Monitoring and Modeling of the Solvent-Mediated Polymorphic Transformation of L-Glutamic Acid. *Cryst. Growth Des.* **2006**, *6*, 881–891.
- [4] de Albuquerque, I.; Mazzotti, M. Crystallization Process Design Using Thermodynamics To Avoid Oiling Out in a Mixture of Vanillin and Water. *Cryst. Growth Des.* **2014**, *14*, 5617–5625.
- [5] Cornel, J.; Lindenberg, C.; Mazzotti, M. Quantitative Application of in Situ ATR-FTIR and Raman Spectroscopy in Crystallization Processes. *Ind. Eng. Chem. Res.* **2008**, *47*, 4870–4882.
- [6] Schorsch, S.; Ochsenein, D. R.; Vetter, T.; Morari, M.; Mazzotti, M. High accuracy online measurement of multidimensional particle size distributions during crystallization. *Chem. Eng. Sci.* **2014**, *105*, 155–168.
- [7] Ochsenein, D. R.; Schorsch, S.; Vetter, T.; Mazzotti, M.; Morari, M. Growth Rate Estimation of β L-Glutamic Acid from Online Measurements of Multidimensional Particle Size Distributions and Concentration. *Ind. Eng. Chem. Res.* **2014**, *53*, 9136–9148.
- [8] Bötschi, S.; Rajagopalan, A. K.; Morari, M.; Mazzotti, M. Feedback Control for the Size and Shape Evolution of Needle-like Crystals in Suspension. I. Concepts and Simulation Studies. *Cryst. Growth Des.* **2018**, DOI: 10.1021/acs.cgd.8b00473.
- [9] Ku, H. H. Notes on the Use of Propagation of Error Formulas. *J. Res. Natl. Bur. Stand., Sect. C* **1966**, *70C*, 263–273.